Geophysical Research Letters

RESEARCH LETTER
10.1029/2021GL096921

Key Points:

- Glider observations are able to integrate physical and biogeochemical processes influencing oxygen depletion in shelf seas
- Mixing and advection replenish respired oxygen in the bottom mixed layer
- The presence of a subsurface oxygen maxima results in larger oxygen fluxes to the bottom mixed layer in summer compared to spring

Supporting Information:

Supporting Information may be found in the online version of this article.

Correspondence to:

C. A. J. Williams,
chwill@noc.ac.uk

Citation:

Williams, C. A. J., Davis, C. E., Palmer, M. R., Sharples, J., & Mahaffey, C. (2022). The three Rs: Resolving respiration robotically in shelf seas. *Geophysical Research Letters*, *49*, e2021GL096921. https://doi.org/10.1029/2021GL096921

Received 5 NOV 2021
Accepted 14 JAN 2022

The Three Rs: Resolving Respiration Robotically in Shelf Seas

C. A. J. Williams[1], C. E. Davis[2], M. R. Palmer[1], J. Sharples[2], and C. Mahaffey[2]

[1]National Oceanography Centre Liverpool, Liverpool, UK, [2]Department of Earth, Ocean and Ecological Sciences, University of Liverpool, Liverpool, UK

Abstract Ocean deoxygenation threatens ocean productivity, carbon cycling and marine ecosystems. Shelf seas are highly dynamic regions, which contributes to their high productivity and also makes monitoring and constraining their oxygen status a challenge. Here, using the temperate Celtic shelf sea (April and July 2015) as a case study, we present high-resolution ocean glider observations of turbulence and biogeochemical parameters, demonstrating the potential of these autonomous platforms for environmental monitoring. We estimate vertical turbulent oxygen fluxes be 25% higher in summer than in spring, due to the presence of subsurface chlorophyll and associated oxygen maxima at the seasonal thermocline. We demonstrate that glider-based estimates were able to constrain similar bottom layer respiration rates as those derived from traditional ship-based measurements. We suggest ocean gliders are useful monitoring tools that can aid sustainable management of shelf sea ecosystems.

Plain Language Summary Oxygen levels in the ocean are decreasing. Oxygen is needed by almost all life in the oceans, thus low oxygen levels can result in dramatic changes to marine ecosystems. The decrease in oxygen levels is particularly alarming in the coastal ocean or "shelf sea" (the region between the land and the deep open ocean), which supports the majority of global fisheries (over 90%). Therefore, there is both an urgent societal and an environmental need to better understand processes influencing oxygen levels in the coastal ocean, such as physical water circulation and mixing, and biological oxygen production and consumption. Here we present turbulent mixing data collected over 40 days in a typical shelf sea using an unmanned, autonomous underwater vehicle (AUV) called an ocean glider. We use this data combined with oxygen data to calculate the contribution of physical oxygen fluxes to the observed change in oxygen, and from this deduce how much of the change was driven by biology. We prove that AUVs may be used as an effective method for monitoring oxygen dynamics and that this can aid responsible marine management in shelf seas.

1. Introduction

The global ocean dissolved oxygen (O_2) inventory is decreasing (Schmidtko et al., 2017) and the areal extent of O_2 deficiency is increasing (Diaz & Rosenberg, 2008; Keeling et al., 2010; Queste et al., 2013). The development or expansion of O_2 deficient regions has the potential to dramatically affect marine habitats, ecology, nutrient cycles and fisheries (Breitburg et al., 2018; Diaz & Rosenberg, 2008; Rabalais et al., 2014), leading to an immediate need to better understand the processes that control the distribution of O_2.

Shallow continental shelf seas (<200 m) are extremely productive regions. While covering only ~7% of the world ocean area, they support more than 90% of global fisheries (Pauly et al., 2002; Young et al., 2001) and primary production rates are 3–5 fold higher than those of the open ocean (Simpson & Sharples, 2012). However, O_2 deficiency is evident in several shelf seas (Diaz & Rosenberg, 2008; Gilbert et al., 2010; Grantham et al., 2004; Greenwood et al., 2010; Queste et al., 2013) with recent model studies (NEMO-ERSEM, Butenschön et al., 2016) estimating that large regions of the Northwest European continental shelf seas (325,000–400,000 km^2) have the potential to become seasonally deficient in O_2 in late summer (Ciavatta et al., 2016) and future climate scenarios (Wakelin et al., 2020). Although hypoxia (O_2 < 2 mg L^{-1}) is never reached, the threat of O_2 deficiency (<6 mg L^{-1}; OSPAR, 2013) is still lethal for some fish and molluscs (Vanquer-Sunyer & Duarte, 2008).

In shelf seas, the surface mixed layer (SML) is well oxygenated due to air-sea gas exchange and net biological production. However, the shelf sea thermocline acts as a physical barrier between the warmer, oxygenated, nutrient deplete SML and the cooler, dark, nutrient rich bottom mixed layer (BML; Figure 1; see also Sharples et al., 2001). In the BML, net O_2 removal can occur as a result of restricted ventilation due to seasonal thermal stratification, oxygen consumption via respiration of organic matter, and nitrification. An important mechanism

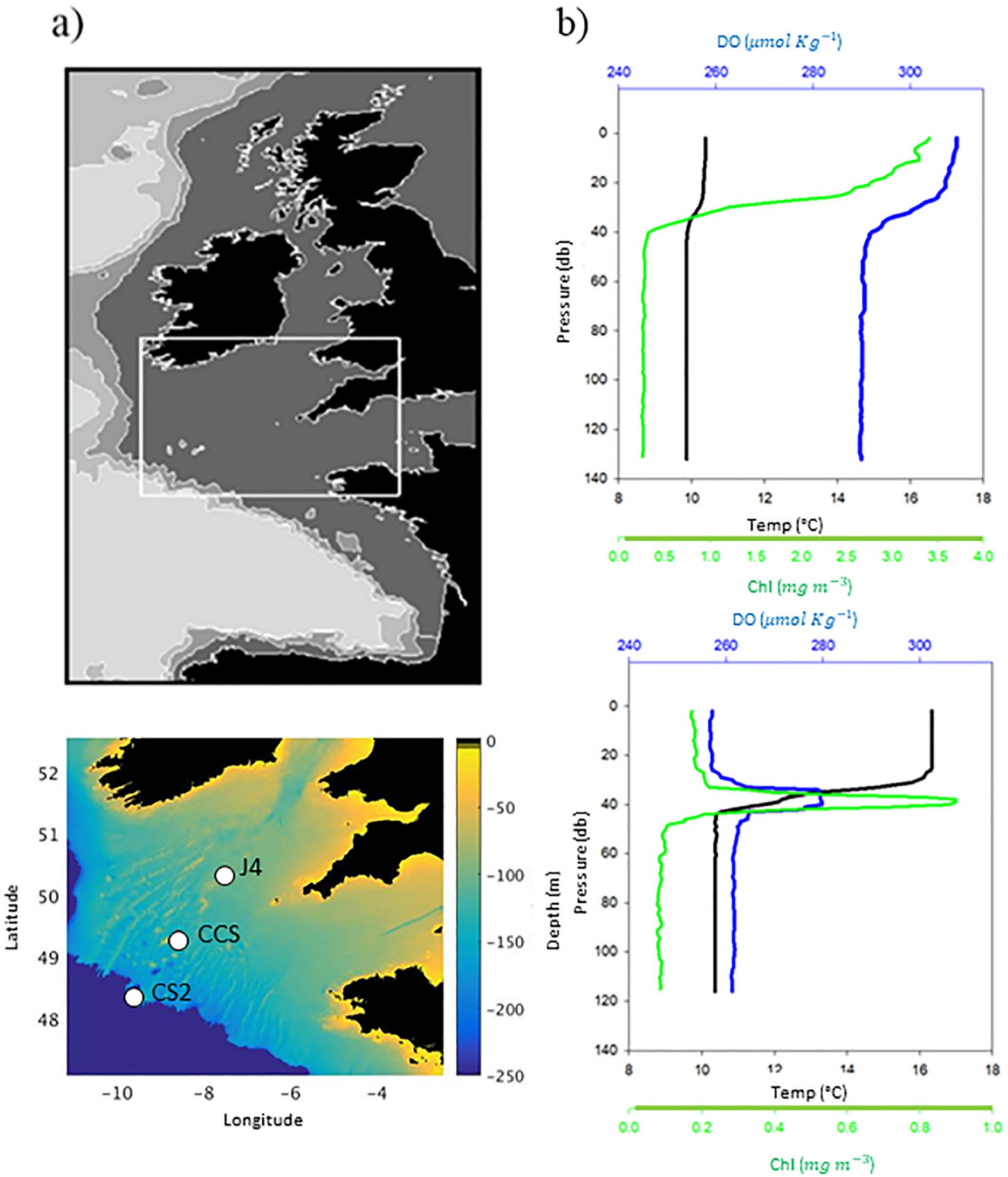

Figure 1. (a) Map of Northwest European shelf with (c) inset showing location of our study site, the Central Celtic Sea (CCS) and additional stations used for horizontal dispersion and advection calculations J4 and CS2. The right hand figures show typical vertical profiles of temperature (°C, black line), chlorophyll (mg m^{-3}; green line) and dissolved oxygen concentration (O_2, µmol kg^{-1}, blue line) during (b) the spring and (d) the summer.

in sustaining high productivity in shelf seas is the diapycnal upward mixing of nutrients across the base of the thermocline barrier (Brandt et al., 2015; Davis et al., 2014; Rippeth, 2005; Rippeth et al., 2014; Williams, Sharples, Green, et al., 2013; Sharples et al., 2007). This mixing is driven by the barotropic tide, internal waves and wind-driven inertial oscillations (Burchard & Rippeth, 2009; Inall et al., 2000; Sharples et al., 2007; Williams, Sharples, Mahaffey, & Rippeth, 2013). There is potential for diapycnal mixing to help alleviate O_2 deficiency in the BML by providing a downward turbulent flux of O_2 across the thermocline (Queste et al., 2016; Rovelli et al., 2016).

Future shelf sea scenarios indicate prolonged, earlier onset of stratification and stronger thermocline stability (Lowe et al., 2009; Meire et al., 2013; Sharples et al., 2013), all of which affects BML ventilation and O_2 dynamics (Wakelin et al., 2020). However, despite the prominence of gathering O_2 data in order to assess the health of shelf seas, these measurements are either seasonally or spatially limited (Große et al., 2016). It is apparent that there is an immediate need for high spatio-temporal resolution O_2 measurements alongside estimates of physical mixing to elucidate the physical and biogeochemical processes that govern the development of O_2 deficiency, enabling effective ecosystem management of shelf seas.

Here, we present a novel data set of autonomously sampled high-resolution O_2 and turbulent dissipation measurements over a 40-day period in the temperate, seasonally stratified Celtic Sea. The Celtic Sea supports a large phytoplankton bloom in spring, strong stratification in summer and a second bloom event in autumn at the breakdown of stratification (Holligan et al., 1984; Pingree et al., 1976, 1978). The impact of vertical exchange across the thermocline on nutrient transfer is already locally well characterized (Davis et al., 2014; Sharples et al., 2001; Williams, Sharples, Mahaffey, & Rippeth, 2013), thus it is a good study site to assess the role of diapycnal mixing on O_2 fluxes and distribution. Using an ocean glider we were able to quantify and assess the diapycnal exchange of O_2 between the SML and BML. Finally, we use these measurements, combined with estimates of the horizontal dispersion and advection, to calculate respiration during spring and summer 2015.

2. Materials and Methods

2.1. Glider Measurements

Ocean gliders were deployed to conduct "virtual mooring" profiles at a study site in the seasonally stratified central Celtic Sea (station CCS, 49° 24' N, 8° 36' W; see Figure 1) during spring 2015 (6th–28th April, decimal day 95–117) and summer 2015 (15th July–2nd August, decimal day 195–213). The integrated approach adopted in this study, combining ship based and glider measurements enabled estimates of spatial gradients while also minimising tidal aliasing that would likely be introduced by long spatial transects with the glider. A Slocum (Teledyne Webb Research, Falmouth, USA) Ocean Microstructure Glider (OMG, see Palmer et al., 2015) was equipped with a MicroRider microstructure package (Rockland Scientific International) to measure the microstructure of velocity shear, a Seabird SBE42 CTD sensor to measure temperature, salinity and pressure, and an Aanderaa 4831 oxygen optode to measure O_2 (precision 0.2 μmol kg^{-1}). Measurements were taken within 5 m of the bed and 2 m of the surface on most dives, with each yo-yo profile taking approximately 20 min. The glider AA4831 optode is known to experience severe lag across strong oxygen gradients, and therefore oxygen data was corrected where possible for optode membrane lag following Bittig et al. (2014). In comparison to other oxygen optodes, the AA4831 has been documented by various scientific studies as being an extremely stable optode with low detectable drift (<0.5% yr^{-1}) and high precision of <0.2 μmol kg^{-1} (Champenois & Borges, 2012; Johnson, 2010; Kortzinger et al., 2004; Nicholson et al., 2008). Optode drift was calculated in this study by comparing discrete Winkler-analyzed samples taken at deployment and recovery of the gliders, identifying a downward drift of 0.001% d^{-1}, in close agreement with quoted manufacturer values.

Glider sensors (temperature, salinity and O_2) were calibrated against nearby ship CTD profiles (CTD calibrated 1 month prior to cruise, SBE 43 precision = 2% of O_2 saturation) and discrete water samples collected within 3 hr and 2 km of glider deployment and recovery times and glider position, respectively, as part of the Shelf Sea Biogeochemistry program (*RRS Discovery*, DY029 and DY033). Error estimates for the total change in $O_{2\ \mathrm{BML}}$ (μmol kg^{-1}) were calculated as the sum of the optode precision (0.2 μmol kg^{-1}) and drift over the entire respective deployments (<0.1 μmol kg^{-1}). Currents were monitored throughout the glider deployments by a mooring at the CCS study site, which was equipped with an acoustic current profiler (ADCP), salinometer and thermistors that provided near-continuous data (Ruiz-Castillo et al., 2019; Wihsgott et al., 2019).

2.2. Oxygen Budget Calculations

The change in $O_{2\ \mathrm{BML}}$ can be represented by the following equation:

$$\frac{dC(O_2)}{dt} = -u\frac{dC(O_2)}{dx} - v\frac{dC(O_2)}{dy} - w\frac{dC(O_2)}{dz} + \frac{K_z\frac{dC(O_2)}{dz}}{Z_{\mathrm{BML}}} + K_h\frac{d^2C(O_2)}{dx^2} - \frac{\Delta C(O_2)}{dt} \quad (1)$$

where C(O_2) represents the concentration of O_2 (μmol kg^{-1}). The term on the LHS refers to the change observed in $O_{2\ \mathrm{BML}}$ over the sampling periods. The first three terms on the RHS represents the advection of water with respect to the x, y (horizontal), and z (vertical) coordinates. The fourth and fifth terms represent the vertical and horizontal turbulent flux of oxygen into the BML respectively, where K_z refers to the vertical eddy diffusivity, K_h refers to the horizontal eddy diffusivity and Z_{BML} represents the thickness of the BML (m). The final term, $\Delta C\ (O_2)$, represents the net effect of biological processes on oxygen. In the BML, this will be the depletion of O_2 due to nitrification and bacterial respiration.

2.2.1. Vertical Diffusivity

Vertical turbulent diffusion (K_z, m^2 s^{-1}), was calculated using profiles of the rate of dissipation of turbulent kinetic energy (TKE; ε, m^2 s^{-3}) and the buoyancy frequency (N^2, s^{-2}) following Equation 2 (e.g., Osborn, 1980):

$$K_z = \Gamma\frac{\varepsilon}{N^2}\left(\mathrm{m^2 s^{-1}}\right) \quad (2)$$

Here Γ, the mixing efficiency, is considered constant at 0.2 for the stratified water column (Osborn, 1980; Tweddle et al., 2013; Williams, Sharples, Green, et al., 2013). While there is ongoing discussion on the assumption of a constant mixing efficiency in stratified fluids, the vast majority of studies have not conclusively arrived at a suitable improvement to that proposed by Osborn (1980), so this simple solution has been employed here as current best practice (Gregg et al., 2018).

The buoyancy frequency was calculated using the density profiles (Equation 3):

$$N^2 = -\frac{g}{\rho}\left(\frac{d\rho}{dz}\right)\left(\mathrm{s^{-2}}\right) \quad (3)$$

where g is the acceleration due to gravity (9.81 m s^{-2}), ρ is density, and z is the vertical coordinate (m, positive upward).

The base of the pycnocline represents the interface for diapycnal mixing and O_2 fluxes and was defined as the depth that marked the top of the BML. We chose this to be where the density decreased by 15% of the total water column density change. This allowed us to standardize our method over various densities during spring and summer.

2.2.2. Vertical O_2 Flux

Vertical turbulent driven fluxes of O_2 from the base of the pycnocline into the BML may be calculated following Equation 4 (e.g., Sharples et al., 2001)

$$J_{O_2} = -K_z\left(\frac{dC(O_2)}{dz}\right)\left(\mathrm{mmol\ m^{-2}s^{-1}}\right) \quad (4)$$

where $\frac{dC(O_2)}{dz}$ represents the vertical gradient in oxygen (mmol m^{-4}) and K_z is the eddy diffusivity defined in Equation 2. Confidence limits (95%) for J_{O_2} were calculated using Efron Gong Bootstrap resampling method (Efron & Gong, 1983).

2.2.3. Horizontal Advection of O_2

The Celtic Sea is bordered by the Northeast Atlantic to the west, St Georges Channel and the Irish Sea to the north, and the Bristol and English Channels to the northeast and east, respectively. Fronts form at each of these boundaries which have the potential to generate eddies that transfer properties (e.g., salt, heat and O_2) and momentum laterally across the shelf (Huthnance et al., 2009; Proctor et al., 2003) before being eroded by wind and tidal mixing (Badin et al., 2010). In the Celtic Sea, internal tides can be large and non-linear resulting in solitons that

can drive on-shelf exchange of oceanic water (Huthnance et al., 2009). In April 2015 and August 2015, oceanic waters moved on-shelf in the bottom layer at 1.4 and 1.5 km d^{-1} respectively, due to wind-driven Ekman transport, cross-shelf pressure gradients and/or internal tidal wave Stokes drift (Ruiz-Castillo et al., 2019). Based on these estimates, shelf edge waters would take 110 and 150 days to travel from the shelf edge to our study site respectively. It is important to note that there are likely large uncertainties in these estimations, however the estimations by Ruiz-Castillo et al. (2019) are still the best measurements of horizontal fluxes in this area. During this period, the bottom layer horizontal oxygen gradient indicated that O_2 concentrations were lowest at the shelf edge and increased with distance on shelf to the highest concentrations at our study site (Figure S1 in Supporting Information S1). This negative on-shelf gradient suggests that water with comparatively lower O_2 concentration would be slowly advected to our study site.

2.2.4. Horizontal Dispersion of O_2

Observations of horizontal dispersion coefficients (K_h) in shelf seas are typically between 10 and 600 $m^2\ s^{-1}$ (Houghton et al., 2009; Sanders & Garvine, 2001). In order to calculate the horizontal dispersion of O_2 the derivative of the lateral gradient in O_2 is needed (Equation 1).

3. Results

3.1. Water Column Characteristics

The onset of thermal stratification at our site in the central Celtic Sea occurred on the 6th April (decimal day 95) coinciding with a period of reduced wind mixing and increased solar heating (Wihsgott et al., 2019). This supported the development of an intense spring bloom occurring between days 95 and 114 (Poulton et al., 2019), where O_2 was relatively high throughout the water column (280–310 μmol kg^{-1}) as a result of increased primary productivity. There was less than 1°C difference between SML and BML temperature, separated by a 30 m thick thermocline (Figure 1a). Tidal currents were 0.2–0.4 ms^{-1} with the fastest currents in the SML (Figures S3 and S4 in Supporting Information S1). The BML temperature at CCS was 2°C warmer than that at the shelf edge (Figure S1 in Supporting Information S1). $O_{2\ BML}$ at CCS was 17.7 μmol kg^{-1} larger than $O_{2\ BML}$ at the shelf edge (Figure S1 in Supporting Information S1) during spring 2015 therefore on-shelf advection in the BML (e.g., Ruiz-Castillo et al., 2019) would have diluted $O_{2\ BML}$ concentrations at our study site.

Stratification was more pronounced in July with the SML being 5°C warmer than the BML (Figure 1c). The vertical gradient in O_2 was also different from spring, with the lowest concentrations in the SML (249 μmol kg^{-1}), then the BML (253 μmol kg^{-1}), and the highest concentrations within the 15 m thick seasonal thermocline (273 μmol kg^{-1}, Figure 1c). Following the depletion of nutrients in the SML, phytoplankton thrive at the base of the pycnocline, where nutrients (mixed up from the BML) and light are available (Sharples et al., 2001). Phytoplankton photosynthesize at the base of the pycnocline, and thus a SCM as well as O_2 maxima, is observed here (Figure 1d). The thermocline and depth of the base of the pycnocline were stronger and deeper, respectively, in summer than in spring, with Z_{BML} decreasing from 95 m in spring to 85 m in summer (Figures 1b and 1c). The vertical oxygen gradient (dO_2/dz) at the base of the pycnocline was more than twice as strong in summer than in spring (Table 1). $O_{2\ BML}$ at CCS was 7 μmol kg^{-1} larger than $O_{2\ BML}$ at the shelf edge (Table 1), indicating a decrease in the across shelf horizontal $O_{2\ BML}$ gradient in summer.

3.2. Vertical Mixing

Highly energetic mixing in the BML and SML was contrasted against the base of the pycnocline, where TKE dissipation (ε; Wm^{-3}), was low, marking the extent of boundary driven turbulence (Simpson et al., 1996, Figure 2c). The OMGs sampled two spring tides and one neap tide during both spring (days 94–96, 108–110, and 101–103, respectively, see Figure S3 in Supporting Information S1) and summer (days 196–198, 210–212, and 203–205, respectively). An ODAS meteorological buoy at the CCS mooring observed near-gale force winds (>13.9 m s^{-1}) on days 107, 204, 206, and 207 (Figure S2 in Supporting Information S1).

The strongest mixing and highest values of K_z at the base of the pycnocline were observed on day 107 ($6.2 \times 10^{-3}\ m^2\ s^{-1}$, Figure 2d), corresponding with near-gale conditions on day 107 (wind speeds >17 m s^{-1}, see Figure S2 in Supporting Information S1) occurring immediately prior to spring tides (day 108–110). Persistent strong winds on days 107–113 (Figure S2 in Supporting Information S1) prolonged strong mixing and a relatively

Table 1
Derived Parameters and Flux Calculations

	April 15	July 15
Z_{BML} (m)	95	85
$dO_{2\ BML}/dt$ (mmol m^{-2} d^{-1})	**−21.9 [±0.3]**	**−8.5 [±0.3]**
K_h (m^2 s^{-1}) Sanders and Garvine (2001); Houghton et al. (2009)	10–600	10–600
$d2O_2/dx^2$ (mmol m^{-5})	1.4×10^{-9}	-34.1×10^{-9}
Horizontal dispersion (mmol m^{-2} d^{-1})	**0.1 to 6.6**	**−0.1 to −1.5**
U (m d^{-1}) Ruiz-Castillo et al. (2019)	1,400	1,500
d O_2/dx (mmol m^{-4})	-15.5×10^{-5}	-6.1×10^{-5}
Horizontal advection (mmol m^{-2} d^{-1})	**−0.2**	**−0.1**
K_z x 10^{-5} (m^{-2} s^{-1})	4.8 [3.4–6.5]	3.1 [2.2–4.0]
K_z Neap/spring	1.2 [0.7 to 1.6] 9.4 [5.0 to 10.5]	0.8 [0.5 to 1.1] 10.4 [4.3 to 19.6]
dO_2/dz (mmol m^{-4})	0.7 [0.6–0.8]	1.5 [1.0–2.0]
Vertical flux J_{O_2} (mmol m^{-2} d^{-1})	**2.9 [1.8 to 4.5]**	**3.9 [1.9 to 6.9]**
J_{O_2} Neap/spring	0.7 [0.4 to 1.1] 5.7 [0.3 to 7.3]	1.0 [0.4 to 1.9] 13.5 [3.7 to 33.9]
Respiration estimate from this study (mmol m^{-2} d^{-1})	**23.9 to 32.9**	**8.6 to 15.4**
Microplankton Community respiration (mmol m^{-2} d^{-1}) Garcia-Martin et al. (2018)	**59.9 [17.1 to 102.7]**	**12.8 [6 to 19.6]**

high oxygen flux beyond the spring-tide period (Figure 2). During summer, high levels of diapycnal K_z exceeding 1.8×10^{-3} m^2 s^{-1} were also observed during spring tides (days 196–198, 210–212; Figure 2d). The lowest values of K_z at the base of the pycnocline were at molecular levels (O (1e-9) m^2 s^{-1}) observed immediately after neap tides, and highest values were observed to coincide with spring tides (Figure 2d).

3.3. Vertical Mixing of O_2

The diapycnal O_2 flux (J_{O_2}) ranged from O (1e-7) to 6.49×10^{-4} mmol m^{-2} s^{-1}, with the highest J_{O_2} (6.49×10^{-4} mmol m^{-2} s^{-1}) being observed during summer (day 211) coinciding with K_z spikes at spring tides. The lowest O_2 fluxes were observed immediately after neap tides concurring with low K_z values.

Average O_2 fluxes across the base of the seasonal pycnocline were higher in July by ∼25%, this was due to the vertical O_2 gradient being twice as strong during July (Table 1). It is important to note that the calculation of K_z (Equation 2) considers a constant mixing efficiency and thus does not take into account the dampening effect of stronger stratification on diapycnal mixing in summer compared to spring, which has been shown in previous studies to potentially affect the vertical flux (Schultze et al., 2017). Fluxes were almost a factor of 10 larger during spring tides than neap tides in both spring and summer driven by enhanced K_z.

3.4. Horizontal Advection and Diffusion of O_2

The horizontal advection of O_2 to our study site was calculated using the values of horizontal advection (Ruiz-Castillo et al., 2019) together with the measured horizontal gradient (dO_2/dx) in the BML for both spring and summer (Figure S1 in Supporting Information S1). The horizontal O_2 gradient from the shelf edge to CCS in the BML was -15.5×10^{-5} mmol m^{-4} during spring, the strength of this gradient reduced in summer to -6.1×10^{-5} mmol m^{-4} (Figure S1 in Supporting Information S1). The horizontal advection of on-shelf waters acted to dilute O_2 at our study site during both spring (−0.2 mmol m^{-2} d^{-1}) and summer (−0.1 mmol m^{-2} d^{-1}).

Using the upper and lower estimates of horizontal dispersion across the shelf of 10–600 (m^2 s^{-1}; Houghton et al., 2009; Sanders & Garvine, 2001), together with the derivative of the lateral gradient ($d2O_2/dx^2$) in the BML from J4 to the shelf edge (Table 1), we were able to quantify the horizontal dispersion of O_2 to our study site. The horizontal dispersion acted as a source of 0.1–6.6 mmol m^{-2} d^{-1} of O_2 to CCS during spring. During July however, the horizontal dispersion acted to dilute the O_2 at our study site by −0.1 to −1.5 mmol m^{-2} d^{-1}.

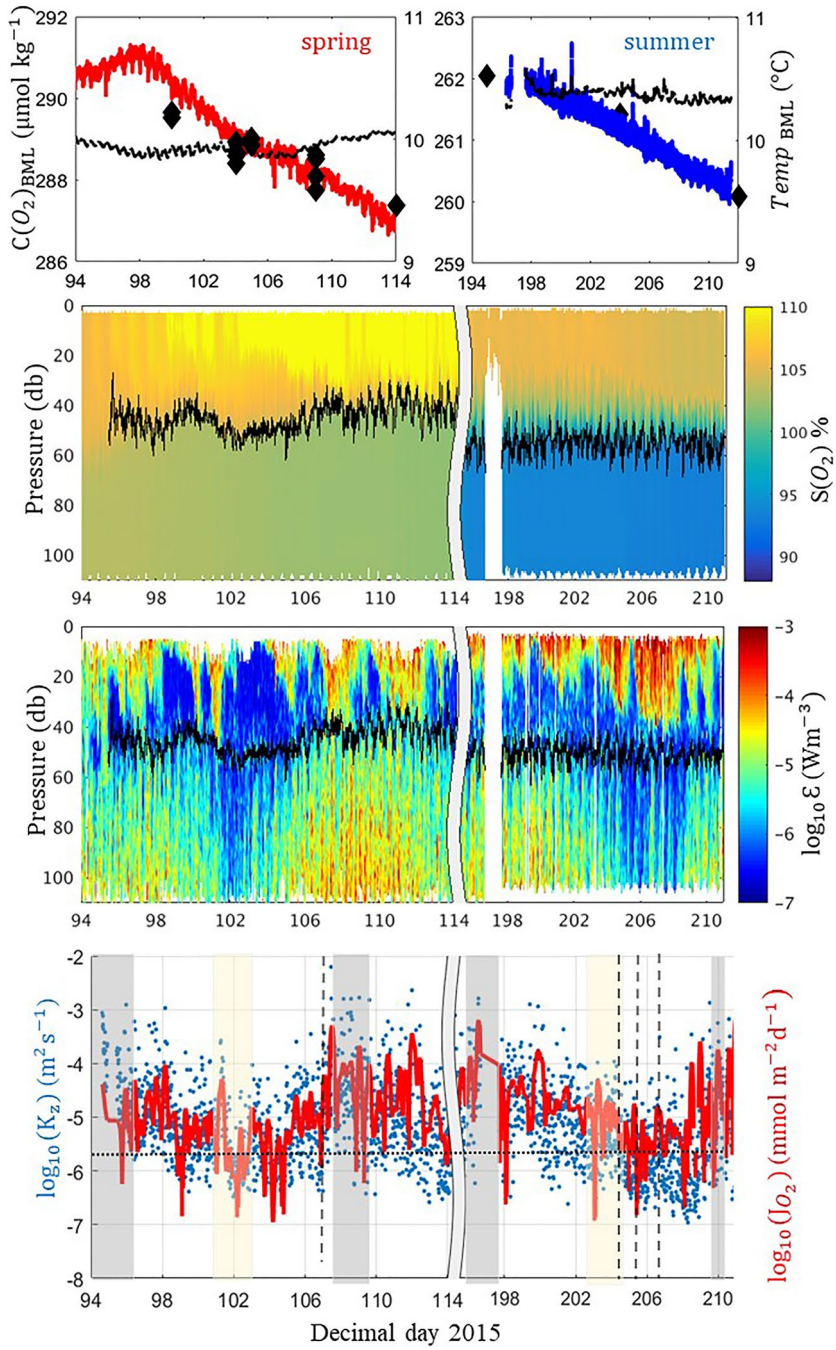

Figure 2. (a) O_2 saturation (%) (b) bottom mixed layer O_2 (µmol kg^{-1}) from spring (red line) and summer (blue line) glider deployments with O_2 from discrete water samples (crosses). (c) Turbulent kinetic energy dissipation, ε (W m^{-3}), measured from the glider. Black lines in (a and c) indicate the base of the pycnocline used for all calculations. (d) K_z at the base of pycnocline (blue dots) with the diapycnal O_2 flux (red line). Spring and neap tide periods have been highlighted by shaded boxes (gray and light yellow respectively), and periods when gale force winds (>13.9 m s^{-1}) occur (black dashed lines). The broken X axis separates the two different glider time series. The horizontal black dotted line marks where the $K_{z\,min}$ threshold for a constant mixing efficiency of 0.2.

3.5. Estimates of Respiration

The net effect of biological processes (ΔC) on $O_{2\ BML}$ during the sampling period can be estimated from the supply rate of O_2 to the BML via the vertical and horizontal fluxes and the *in situ* $O_{2\ BML}$ concentrations measured

by the gliders (rearranging Equation 1). Once the BML was isolated from direct air-sea gas exchange by stratification, there was no change in O_2 concentration due to reduced gas solubility associated with the increase in BML temperature of 0.003°C d^{-1} (Figure 2a). During the two separate glider sampling periods, the depth-integrated $O_{2_{BML}}$ was observed to decrease at a rate of -28.5 ± 0.10 mmol m^{-2} d^{-1} in spring (decimal days 95–114), and -8.5 ± 0.09 mmol m^{-2} d^{-1} in summer (decimal days 193–212), with O_2 saturation in the BML reaching 92% by decimal day 234 (Figure 2). Rearranging Equation 1, the depth-integrated ΔC was estimated to be in the range 23.9–32.9 mmol m^{-2} d^{-1} in spring and 8.6–15.4 mmol m^{-2} d^{-1} in summer, indicating net consumption of O_2 in the BML during both periods.

4. Discussion and Conclusions

Oxygen decline is evident in several shelf seas, with large regions of the Northwest European continental shelf seas having the potential to become seasonally deficient in $\boldsymbol{O_2}$ in late summer under current conditions (Ciavatta et al., 2016) and more extensively under future predicted climate scenarios (Wakelin et al., 2020). In this study, using a novel high-resolution data set collected using ocean gliders, we accurately balanced the $\boldsymbol{O_2}$ inventory in the central region of a broad, stratified shelf sea.

Our high resolution glider-based O_2 measurements in the Celtic Sea were in good agreement with nearby ship-based CTD measurements. For example, mean BML O_2 concentrations from the glider were 289 ± 2 µmol kg^{-1} in spring and 261 ± 2 µmol kg^{-1} in summer, respectively, with equivalent values from the CTD of 289 ± 1 and 261 ± 1 µmol kg^{-1}, respectively. Error estimates for the total change in $O_{2\ \mathrm{BML}}$ (µmol kg^{-1}) were calculated as the sum of the optode precision (0.2 µmol kg^{-1}) and drift (<0.1 µmol kg^{-1}) over the entire respective deployments ($\pm$0.3 µmol kg^{-1}). Good agreement between our K_z values at the base of the seasonal pycnocline and those previously reported for the Celtic Sea (Palmer et al., 2013; Williams, Sharples, Mahaffey, & Rippeth, 2013) and other temperate shelf seas (e.g., Mackinnon & Gregg, 2003) suggests that we obtained accurate K_z measurements at high spatial and temporal resolution during our study. A caveat of our method is that the calculation of K_z (Equation 2) considers a constant mixing efficiency and thus does not take into account the dampening effect of stronger stratification on diapycnal mixing in summer compared to spring, which has been shown in previous studies to potentially affect the vertical flux (Schultze et al., 2017). There is no consensus for a constant mixing efficiency there is agreement that below a certain buoyancy Reynolds number (Re_b) turbulence is not mixing diapycnally (Schultze et al., 2017), thus Equation 2 would be valid only in developed turbulence. If we compute the minimum diffusivity ($K_{z\,\mathrm{min}}$) of an isotropic turbulence patch using $\mathrm{Re}_b > 7$ to (Schultze et al., 2017), this gives a $K_{z\,\mathrm{min}}$ value of $\sim 1.4 \times 10^{-6}$ m^2 s^{-1} (Figure 2d, dashed line). Only a small number of diffusivities fall below this (Figure 2d), indicating that a constant mixing efficiency of 0.2 is suffice for the majority of our study, but in low energy environments our method of calculating the vertical O_2 flux might not hold.

Diapycnal mixing in temperate shelf seas maintains the ecosystem in a variety of ways; (a) supplying nutrients to the euphotic zone (Sharples et al., 2001, 2007, Williams, Sharples, Green, et al., 2013, Williams, Sharples, Mahaffey & Rippeth, 2013), (b) supplying organic matter to the BML (Davis et al., 2014, 2018); (c) supplying O_2 to the BML (Rovelli et al., 2016). Downward O_2 fluxes were largest during spring tides, with fluxes increasing 8-fold in spring and 13-fold in summer (Table 1) relative to neap periods. Despite similar K_z values, O_2 fluxes were more 25% larger during summer than spring due to a stronger $\frac{dC(O_2)}{dz}$ gradient associated with the oxygen maximum (Figures 1b and 1c; Table 1). During high wind conditions (>14 ms^{-1}) spring tide O_2 fluxes were still a factor of 10 larger than during neap tide under similar wind conditions (e.g., 50×10^{-5} mmol m^{-2} s^{-1} and 0.4×10^{-5} mmol m^{-2} s^{-1}, respectively, on days 107 and 204, Figure 2d, Figure S1 in Supporting Information S1). These O_2 fluxes were significantly smaller than values measured over a 3 days study in the North Sea by Rovelli et al. (2016) (~54 mmol m^{-2} d^{-1}), which were comparable to the biological consumption of O_2 in the BML (~60 mmol m^{-2} d^{-1}). Conversely, in our study, it appears that J_{O_2} provides a steady leakage of O_2 into the BML which is smaller than ΔC indicating that J_{O_2} is not enough to sustain the biological O_2 demand but does act to slow the rate of $O_{2\ \mathrm{BML}}$ depletion in the BML. A recent study concluded that the vertical downward mixing of O_2 was not sufficient to maintain the hypoxic transition zone of the Baltic Sea (Holtermann et al., 2020). In contrast to our study, horizontal intrusions were an important O_2 source in the Baltic.

Water of lower O_2 concentration was advected from the shelf edge to our study site and was twice as strong in spring than summer (0.2 and 0.1 mmol m^{-2} d^{-1} respectively). This seasonal difference was due to the horizontal gradient

across the shelf in O_2 being stronger in spring than summer (-15.5×10^{-5} mmol m^{-4} and -6.1×10^{-5} mmol m^{-4} respectively). The greater lateral O_2 gradient during spring was partly due to a supersaturated BML at CCS following the spring bloom (Figure S1b in Supporting Information S1). Our measurements indicated that O_2 consumption by biological processes occurs in the BML in both spring and summer, with the estimated ΔC being 3-fold higher in spring compared to summer (68 ± 0.1 mmol m^{-2} d^{-1} and 20 ± 0.1 mmol m^{-2} d^{-1}, respectively, Table 1). Elevated O_2 consumption in the BML during spring likely reflect the higher availability of organic matter for remineralization via downward sinking particles and fresher dissolved organic matter in spring relative to summer (Davis et al., 2018; Garcia-Martin et al., 2018). Our estimates of net O_2 consumption are in good agreement with community respiration rates reported by Garcia-Martin et al. (2018) at the same study site during spring and summer (36–133 mmol m^{-2} d^{-1} and 9–26 mmol m^{-2} d^{-1}, respectively; Table 1). Our findings suggest that BML respiration rates can be accurately estimated using this method of combined glider and ship-based observations, providing insight into the importance of various consumption processes on BML O_2.

The results we have presented of high resolution shelf sea O_2 distribution and vertical diffusivity have only been possible by using ocean gliders, capable of measuring over long periods and during varying sea states that would be problematic from a research vessel. Our results show that diapycnal mixing supplies O_2 to the BML over the pycnocline, varying relative to tides and wind events and modulated by the strength of vertical O_2 stratification. Modifications to these controls has the potential to have important consequences for marine ecosystem health in shelf seas. Future IPCC climate scenarios predict an increase in water temperature, stronger and more prolonged stratification (Lowe et al., 2009), and reduced O_2 concentrations in the BML in shelf seas (Schmidtko et al., 2017; Wakelin et al., 2020). Diapycnal O_2 fluxes observed in this study may become a critical mechanism aiding the ventilation of the BML, helping mitigate O_2 deficiency on continental shelf seas and coastal regions.

Data Availability Statement

All data are publicly available via zenodo (FAIR compliant) with the DOI (https://doi.org/10.5281/zenodo.5914369) under the NERC Open Government License.

Acknowledgments
We thank the captains and crew of the *RRS Discovery* for their help and support at sea and all the scientists involved in the three cruises. We would also like to thank the Marine Autonomous & Robotics Systems (MARS) facility (National Oceanographic Centre, Liverpool) for deployment, recovery and piloting of the gliders, Elena Garcia-Martin for assistance and discussion of respiration estimates. We are grateful to the UK Natural Environment Research Council (NERC) for funding the research cruises via the Shelf Sea Biogeochemistry program and the CANDYFLOSS project that supported this work (NERC grant reference NE/K002007/1).

References

Badin, G., Williams, R. G., & Sharples, J. (2010). Water mass transformation in shelf seas. *Journal of Marine Research*, *68*(2). https://doi.org/10.1357/002224010793721442

Bittig, H. C., Fiedler, B., Scholz, R., Krahmann, G., & Kortzinger, A. (2014). Time dependence on flow speed and temperature. *Limnology and Oceanography: Methods*, *12*, 617–636. https://doi.org/10.4319/lom.2014.12.617

Brandt, P., Bange, H. W., Banyte, D., Dengler, M., Didwischus, S.-H., Fischer, T., et al. (2015). On the role of circulation and mixing in the ventilation of oxygen minimum zones with a focus on the eastern tropical North Atlantic. *Biogeosciences*, *12*, 489–512. https://doi.org/10.5194/bg-12-489-2015

Breitburg, B., Levin, L., Oschlies, A., Gregoire, M., Chavez, F., Conley, D. J., et al. (2018). Declining oxygen in the global ocean and coastal waters. *Science*, *359*, 6371. https://doi.org/10.1126/science.aam7240

Burchard, H., & Rippeth, T. P. (2009). Generation of bulk shear spikes in shallow stratified tidal seas. *Journal of Physical Oceanography*, *39*(4). https://doi.org/10.1175/2008jpo4074.1

Butenschön, M., Clark, J., Aldridge, J., Allen, I. J., Artoli, Y., Blackford, J., et al. (2016). ERSEM 15.06: A generic model for marine biogeochemistry and the ecosystem dynamics of the lower trophic levels. *Geoscientific Model Development*, *57*(1), 347–361. https://doi.org/10.4319/lo.2012.57.1.0347

Champenois, W., & Borges, A. V. (2012). Seasonal and interannual variations of community metabolism rates of a Posidonia oceanica seagrass meadow. *Limnology and Oceanography*, *9*, 1293–1339. https://doi.org/10.5194/gmd-9-1293-2016

Ciavatta, S., Kay, S., Saux-Picart, S., Butenschön, M., & Allen, J. I. (2016). Decadal reanalysis of biogeochemical indicators and fluxes in the North West European shelf-sea ecosystem. *Journal of Geophysical Research: Oceans*, *121*(3). https://doi.org/10.1002/2015jc011496

Davis, C. E., Blackbird, S., Wolff, G., Woodward, M., & Mahaffey, C. (2018). Seasonal organic matter dynamics in a temperate shelf sea. *Progress in Oceanography*. https://doi.org/10.1016/j.pocean.2018.02.021

Davis, C. E., Mahaffey, C., Wolff, G. A., & Sharples, J. (2014). A storm in a shelf sea: Variation in phosphorus distribution and organic matter stoichiometry. *Geophysical Research Letters*. https://doi.org/10.1002/2014gl061949

Diaz, R. J., & Rosenberg, R. (2008). Spreading dead zones and consequences for marine ecosystems. *Science*, *321*(5891), 926–929. https://doi.org/10.1126/science.1156401

Efron, B., & Gong, G. (1983). A leisurely look at the bootstrap, the jackknife, and cross-validation. *The American Statistician*, *37*(1), 36–48. https://doi.org/10.2307/2685844

García-Martín, E. E., Daniels, C. J., Davidson, K., Davis, C. E., Mahaffey, C., Mayers, K. M., et al. (2018). Seasonal changes in plankton respiration and bacterial metabolism in a temperate shelf sea. *Progress in Oceanography*, *177*, 101884. https://doi.org/10.1016/j.pocean.2017.12.002

Gilbert, D., Rabalais, N. N., Diaz, R. J., & Zhang, J. (2010). Evidence for greater oxygen decline rates in the coastal ocean than in the open ocean. *Biogeosciences*, *7*, 2283–2296. https://doi.org/10.5194/bg-7-2283-2010

Grantham, B. A., Chan, F., Nielsen, K. J., Fox, D. S., Barth, J. A., Huyer, A., et al. (2004). Upwelling-driven nearshore hypoxia signals ecosystem and oceanographic changes in the northeast Pacific. *Nature*, *429*, 749–754. https://doi.org/10.1038/nature02605

Greenwood, N., Parker, E. R., Fernand, L., Sivyer, D. B., Weston, K., Painting, S., et al. (2010). Detection of low bottom water concentrations in the Nort Sea; implications for monitoring and assessment of ecosystem health. *Biogeosciences*, *7*, 1357–1373. https://doi.org/10.5194/bg-7-1357-2010

Gregg, M. C., D'Asaro, E. A., Riley, J. J., & Kunze, E. (2018). Mixing efficiency in the ocean. *Annual Review of Marine Science*, *10*, 443–473. https://doi.org/10.1146/annurev-marine-121916-063643

Große, F., Greenwood, N., Kreus, M., Lenhart, H., Machoczek, D., Pätsch, J., et al. (2016). Looking beyond stratification: A model-based analysis of the biological drivers of oxygen deficiency in the North Sea. *Biogeosciences*, *13*, 2511–2535. https://doi.org/10.5194/bg-13-2511-2016

Holligan, P. M., leB Williams, P. J., Purdie, D., & Harris, R. P. (1984). Photosynthesis, respiration and nitrogen supply of plankton populations in stratified, frontal and tidally mixed shelf waters. *Marine Ecology Progress Series*, *17*, 201–213. https://doi.org/10.3354/meps017201

Holtermann, P., Prien, R., Naumann, M., & Umlauf, L. (2020). Interleaving of oxygenized intrusions into the Baltic Sea redoxcline. *Limnology & Oceanography*, *65*, 482–503. https://doi.org/10.1002/lno.11317

Houghton, R. W., Vaillancourt, R. D., Marra, J., Hebert, D., & Hales, B. (2009). Cross-shelf circulation and phytoplankton distribution at the summertime New England shelf break front. *Journal of Marine Systems*, *78*, 411–425. https://doi.org/10.1016/j.jmarsys.2008.11.023

Huthnance, J. M., Holt, J. T., & Wakelin, S. L. (2009). Deep ocean exchange with west-European shelf sea. *Ocean Science*, *5*, 621–634. https://doi.org/10.5194/os-5-621-2009

Inall, M. E., Rippeth, T. J., & Sherwin, T. J. (2000). Impact of nonlinear waves on the dissipation of internal tidal energy at a shelf break. *Journal of Geophysical Research*, *105*(C4), 8687–8705. https://doi.org/10.1029/1999jc900299

Johnson, K. (2010). Simultaneous measurements of nitrate, oxygen, and carbon dioxide on oceanographic moorings: Observing the Redfield ratio in real time. *Limnology & Oceanography*, *55*(2), 615–627. https://doi.org/10.4319/lo.2010.55.2.0615

Keeling, R. F., Körtzinger, A., & Gruber, N. (2010). Ocean deoxygenation in a warming world. *Annual Review of Marine Science*, *2*, 199–229. https://doi.org/10.1146/annurev.marine.010908.163855

Körtzinger, A., Schimanski, J., Send, U., & Wallace, D. (2004). The ocean takes a deep breath. *Science*, *306*(5700), 1337. https://doi.org/10.1126/science.1102557

Lowe, J. A., Howard, T., Pardaens, A., Tinker, J., Holt, J., Wakelin, S., et al. (2009). *UK climate projections science report: Marine and coastal projections*. Retrieved From http://ukclimateprojections.defra.gov.uk/images/stories/marine_pdfs/UKP09_Marine_ report.pdf

Mackinnon, J. A., & Gregg, M. C. (2003). Shear and baroclinic energy flux on the summer New England Shelf. *Journal of Physical Oceanography*, *33*, 1462–1475. https://doi.org/10.1175/1520-0485(2003)033<1462:SABEFO>2.0.CO;2

Meire, L., Soetaert, K. E. R., & Meysman, F. J. R. (2013). Impact of global change on coastal oxygen dynamics and risk of hypoxia. *Biogeosciences*, *10*, 2633–2653. https://doi.org/10.5194/bg-10-2633-2013

Nicholson, D., Emerson, S., & Eriksen, C. C. (2008). Net community production in the deep euphotic zone of the subtropical North Pacific gyre from glider surveys. *Limnology and Oceanography*, *53*(5). 2226–2236. https://doi.org/10.4319/lo.2008.53.5_part_2.2226

Osborn, T. R. (1980). Estimates of the local rate of vertical diffusion from dissipation measurements. *Journal of Physical Oceanography*, *10*(1), 83–89. https://doi.org/10.1175/1520-0485(1980)010<0083:EOTLRO>2.0.CO;2

OSPAR Commission. (2013). *Rules and procedures of the OSPAR commission (Reference Number: 2013-02)*. Retrieved From http://www.ospar.org/documents/dbase/decrecs/agreements/13-02e_rules%20of%20procedure.doc

Palmer, M. R., Inall, M. E., & Sharples, J. (2013). The physical oceanography of Jones Bank: A mixing hotspot in the Celtic Sea. *Progress in Oceanography*, *117*, 57–69. https://doi.org/10.1016/j.pocean.2013.06.009

Palmer, M. R., Stephenson, G. R., Inall, M. E., Balfour, C., Düsterhus, A., & Green, J. A. M. (2015). Turbulence and mixing by internal waves in the Celtic Sea determined from ocean glider microstructure measurements. *Journal of Marine Systems*, *144*, 57–69. https://doi.org/10.1016/j.jmarsys.2014.11.005

Pauly, D., Christensen, V., Guenette, S., Pitcher, T. J., Sumaila, U. R., Walters, C. J., et al. (2002). Towards sustainability in world fisheries. *Nature*, *418*, 689–695. https://doi.org/10.1038/nature01017

Pingree, R. D., Holligan, P. M., & Mardell, G. T. (1978). The effects of vertical stability on phytoplankton distributions in the summer on the northwest European Shelf. *Deep-Sea Research*, *25*(11), 1011–1028. https://doi.org/10.1016/0146-6291(78)90584-2

Pingree, R. D., Holligan, P. M., Mardell, G. T., & Head, R. N. (1976). The influence of physical stability on spring, summer and autumn phytoplankton blooms in the Celtic Sea. *Journal of the Marine Biological Association of the United Kingdom*, *56*, 845–873. https://doi.org/10.1017/s0025315400020919

Poulton, A. J., Davis, C. E., Daniels, C. J., Mayers, K. M. J., Harris, C., Tarran, G. A., et al. (2019). Seasonal phosphorus and carbon dynamics in a temperate shelf sea (Celtic Sea). *Progress in Oceanography*, *177*, 101872. https://doi.org/10.1016/j.pocean.2017.11.001

Proctor, R., Holt, J. T., Allen, J. I., & Blackford, J. (2003). Nutrient fluxes and budgets for the North West European Shelf from a three dimensional model. *Science of the Total Environment*, *314–316*, 769–785. https://doi.org/10.1016/s0048-9697(03)00083-4

Queste, B. Y., Fernand, L., Jickells, T. D., & Heywood, K. J. (2013). Spatial extent and historical context of North Sea oxygen depletion in August 2010. *Biogeochemistry*, *113*(1–3), 53–68. https://doi.org/10.1007/s10533-016-0258-9

Queste, B. Y., Fernand, L., Jickells, T. D., Heywood, K. J., & Hind, A. J. (2016). Drivers of summer oxygen depletion in the central North Sea. *Biogeosciences*, *13*, 1209–1222. https://doi.org/10.5194/bg-13-1209-2016

Rabalais, N. N., Cai, W.-J., Carstensen, J., Fry, B., Hu, X., Zhang, J., et al. (2014). Eutrophication-driven deoxygenation in the coastal ocean. *27*(1), 172–183. https://doi.org/10.5670/oceanog.2014.21

Rippeth, T. P. (2005). Mixing in seasonally stratified shelf seas: A shifting paradigm. *Philosophical Transactions of the Royal Society A: Mathematical, Physical and Engineering Sciences*, *363*(1837), 2837–2854. https://doi.org/10.1098/rsta.2005.1662

Rippeth, T. P., Lincoln, B. J., Kennedy, H. A., Palmer, M. R., Sharples, J., & Williams, C. A. J. (2014). Impact of vertical mixing on sea surface pCO_2 in temperate seasonally stratified shelf seas. *Journal of Geophysical Research: Oceans*, *119*(6), 3868–3882. https://doi.org/10.1002/2014jc010089

Rovelli, L., Dengler, M., Schmidt, M., Sommer, S., Linke, P., & McGinnis, D. F. (2016). Thermocline mixing and vertical oxygen fluxes in the stratified central North Sea. *Biogeosciences*, *13*, 1609–1620. https://doi.org/10.5194/bg-13-1609-2016

Ruiz-Castillo, E., Sharples, J., Hopkins, J., & Woodward, M. (2019). Seasonality in the cross-shelf physical structure of a temperate shelf sea and the implications for nitrate supply. *Progress in Oceanography*, *177*. https://doi.org/10.1016/j.pocean.2018.07.006

Sanders, T. M., & Garvine, R. W. (2001). Freshwater delivery to the continental shelf and subsequent mixing: An observational study. *Journal of Geophysical Research*, *106*(C11), 27087–27101. https://doi.org/10.1029/2001jc000802

Schmidtko, S., Stramma, L., & Visbeck, M. (2017). Decline in global oceanic oxygen content during the past five decades. *Nature*, *542*, 335–339. https://doi.org/10.1038/nature21399

Schultze, L. K. P., Merckelbach, L. M., & Carpenter, J. R. (2017). Turbulence and mixing in a Shallow shelf sea from underwater gliders. *Journal of Geophysical Research: Oceans*, *122*, 9092–9109. https://doi.org/10.1002/2017jc012872

Sharples, J., Holt, J., & Dye, S. (2013). Impacts of climate change on shelf sea stratification. *MCCIP Science Review*, 67–70. https://doi.org/10.14465/2013.arc08.067-070

Sharples, J., Moore, C. M., Rippeth, T. P., Holligan, P. M., Hydes, D. J., Fisher, N. R., & Simpson, J. (2001). Phytoplankton distribution and survival in the thermocline. *Limnology & Oceanography*, *46*, 486–496. https://doi.org/10.4319/lo.2001.46.3.0486

Sharples, J., Tweddle, J. F., Green, J. A. M., Palmer, M. R., Kim, Y., Hickman, A. E., et al. (2007). Spring-neap modulation of internal tide mixing and vertical nitrate fluxes at a shelf edge in summer. *Limnology & Oceanography*, *52*, 1735–1747. https://doi.org/10.4319/lo.2007.52.5.1735

Simpson, J. H., Crawford, W. R., Rippeth, T. P., Campbell, A. R., & Cheok, J. V. S. (1996). The vertical structure of turbulent dissipation in shelf seas. *Journal of Physical Oceanography*, *26*(8), 1579–1590. https://doi.org/10.1175/1520-0485(1996)026<1579:tvsotd>2.0.co;2

Simpson, J. H., & Sharples, J. (2012). *Introduction to the physical and biological oceanography of shelf seas* (p. 448). Cambridge University Press.

Tweddle, J. F., Sharples, J., Palmer, M. R., Davidson, K., & McNeill, S. (2013). Enhanced nutrient fluxes at the shelf sea seasonal thermocline caused by stratified flow over a bank. *Progress in Oceanography*, *117*, 37–47. https://doi.org/10.1016/j.pocean.2013.06.018

Vanquer-Sunyer, R., & Duarte, C. M. (2008). Thresholds of hypoxia for marine biodiversity. *Proceedings of the National Academy of Sciences*, *105*(40), 15452–15457. https://doi.org/10.1073/pnas.0803833105

Wakelin, S., Artioli, Y., Holt, J. T., Butenschon, M., & Blackford, J. (2020). Controls on near-bed oxygen concentration on the Northwest European Continental Shelf under a potential future climate scenario. *Progress in Oceanography*, *187*, 102400. https://doi.org/10.1016/j.pocean.2020.102400

Wihsgott, J. U., Sharples, J., Hopkins, J., Woodward, M. S., Hull, T., Greenwood, N., & Sivyer, D. (2019). Observations of vertical mixing in autumn and its effect on the autumn phytoplankton bloom. *Progress in Oceanography*, *177*, 102059. https://doi.org/10.1016/j.pocean.2019.01.001

Williams, C. A. J., Sharples, J., Green, M., Mahaffey, C., & Rippeth, T. (2013). The maintenance of the subsurface chlorophyll maximum in the stratified western Irish Sea. *Limnology and Oceanography: Fluids and Environments*, *3*(1), 61–73. https://doi.org/10.1215/21573689-2285100

Williams, C. A. J., Sharples, J., Mahaffey, C., & Rippeth, T. (2013). Wind-driven nutrient pulses to the subsurface chlorophyll maximum in seasonally stratified shelf seas. *Geophysical Research Letters*, *40*(20), 5467–5472. https://doi.org/10.1002/2013gl058171

Young, J. W., Bradford, R., Lamb, T. D., Clementson, L. A., Kloser, R., & Galea, H. (2001). Yellowfin tuna (*Thunnus albacares*) aggregations along the shelf break off south-eastern Australia: Links between inshore and offshore processes. *Marine and Freshwater Research*, *52*(4), 463–474. https://doi.org/10.1071/mf99168